HARC as an open-shell strategy to bypass oxidative addition in Ullmann–Goldberg couplings

Marissa N. Lavagnino[a], Tao Liang[a], and David W. C. MacMillan[a,1]

[a]Merck Center for Catalysis, Department of Chemistry, Princeton University, Princeton, NJ 08544

Contributed by David W. C. MacMillan, July 8, 2020 (sent for review June 11, 2020; reviewed by Scott J. Miller and F. Dean Toste)

The copper-catalyzed arylation of unsaturated nitrogen heterocycles, known as the Ullmann–Goldberg coupling, is a valuable transformation for medicinal chemists, providing a modular disconnection for the rapid diversification of heteroaromatic cores. The utility of the coupling, however, has established limitations arising from a high-barrier copper oxidative addition step, which often necessitates the use of electron-rich ligands, elevated temperatures, and/or activated aryl electrophiles. Herein, we present an alternative aryl halide activation strategy, in which the critical oxidative addition (OA) mechanism has been replaced by a halogen abstraction–radical capture (HARC) sequence that allows the generation of the same Cu(III)-aryl intermediate albeit via a photoredox pathway. This alternative mechanistic paradigm decouples the bond-breaking and bond-forming steps of the catalytic cycle to enable the use of many previously inert aryl bromides. Overall, this mechanism allows access to both traditional C–N adducts at room temperature as well as a large range of previously inaccessible Ullmann–Goldberg coupling products including sterically demanding *ortho*-substituted heteroarenes.

photoredox catalysis | C–N coupling | halogen atom abstraction

The arylation of nitrogen nucleophiles has found broad application in many synthetic fields, including materials science, medicinal chemistry, and natural product synthesis (1, 2). While the development of nitrogen arylation protocols has been recently dominated by palladium catalysis (3, 4), the first stoichiometric (5) and catalytic (6) systems reported over a century ago employed copper, an abundant and inexpensive first-row transition metal. The "Ullmann–Goldberg" coupling was limited for many years by the need for high reaction temperatures, stoichiometric copper, and activated electrophiles (e.g., aryl iodides) (7). Notably, the work of Buchwald and others led to the development of chelating diamine ligands (8–10) that prevent nucleophile aggregation on copper, which in turn has enabled milder reaction conditions and broader scope (11). Recent work by Fu and Peters has also shown that direct reduction of the aryl halide by photoexcited, nucleophile-ligated copper complexes is an alternative strategy for aryl halide activation by copper (12, 13). However, a general, copper-catalyzed C(sp^2)–N_{het} Ullmann–Goldberg coupling remains to be developed with respect to aryl position diversity and temperature burden, both critical requirements for the early-stage diversification of pharmaceutically relevant molecules. Recent mechanistic studies have attributed these deficiencies to a high-barrier oxidative addition (OA) step between the electronegative copper(I) catalyst and the aryl halide coupling partner (Fig. 1*A*) (14, 15), a pathway that traditionally demands elevated thermal exposure. Moreover, this step is often prohibitive with *ortho*-substituted aryl bromides due to both steric and electronic factors, a barrier that appears surmountable only via the use of copper-chelating substituents or directing groups (7). With these considerations in mind, we recently sought to develop an alternative mechanistic paradigm that would alleviate the challenge of oxidative addition with copper(I) salts across many reaction classes, while retaining the unique capacity of copper(III) to rapidly undergo reductive elimination (Fig. 1*B*). Herein, we report a photocatalytic approach to the Ullmann–Goldberg coupling that allows a broad range of *para*-, *meta*-, and *ortho*-substituted aryl rings to readily undergo heteroarylation, while achieving high levels of reaction efficiency under ambient or low temperature control.

Over the past 6 years, metallaphotoredox has become a broadly employed strategy for merging photocatalyst-derived organic radicals with transition-metal cycles (16). A fundamental advantage of metallaphotoredox has been that feedstock substrates bearing native functional groups, such as carboxylic acids, amines, alcohols, and C–H bonds, can be converted to high-energy, open-shell intermediates that rapidly participate in transition-metal capture (16). This step has been exploited broadly in the realm of nickel and copper catalysis to deliver a series of new fragment coupling pathways that include deoxygenative C(sp^3)-arylation (17), decarboxylative C(sp^3)-arylation (18), decarboxylative C(sp^3)-amination (19), as well as hydrogen atom transfer (HAT) C(sp^3)-trifluoromethylation (20). In the latter two cases, these copper-based couplings take advantage of 1) Cu(II)'s capacity to capture alkyl radicals at near-diffusion rates (21, 22) and 2) Cu(III)'s established propensity to undergo reductive elimination (RE) steps that are traditionally difficult for more commonly utilized metal catalysts (23).

Among numerous strategies to access alkyl and aryl radicals via photoredox, perhaps the most commonly employed within the pharmaceutical sciences has been halide abstraction from C(sp^3)–Br and C(sp^2)–Br moieties using photogenerated, electron-rich silyl radicals (24–27). In particular, the nickel-catalyzed cross-electrophile coupling to forge C(sp^3)–C(sp^2) bonds via a halogen abstraction–radical capture (HARC) mechanism has been adopted broadly due to its remarkable scope and functional group tolerance (28). This silyl-mediated HARC mechanism has also been interfaced recently with copper catalysis to enable the incorporation of moieties that are

Significance

Copper-catalyzed carbon–nitrogen bond formation has the potential to provide efficient synthetic access to medicinally relevant organic molecules, but broad use of the coupling has been hampered by the requirement for an energetically challenging substrate activation step (oxidative addition into an aryl halide). Here we report a mechanistic alternative that circumvents oxidative addition by cooperatively employing photochemically generated silicon-centered radicals and copper to activate aryl halides via a one-electron pathway. This dramatically increases the range of accessible products, thereby allowing room-temperature synthesis of a diverse electronic and steric range of products traditionally considered inaccessible via copper catalysis due to the prohibitively high barrier for direct copper oxidative addition.

Author contributions: M.N.L., T.L., and D.W.C.M. designed research; M.N.L. and T.L. performed research; M.N.L., T.L., and D.W.C.M. analyzed data; and M.N.L. and D.W.C.M. wrote the paper.

Reviewers: S.J.M., Yale University; and F.D.T., University of California, Berkeley.

Competing interest statement: D.W.C.M. declares a competing financial interest with respect to the Integrated Photoreactor.

[1]To whom correspondence may be addressed. Email: dmacmill@princeton.edu.

This article contains supporting information online at https://www.pnas.org/lookup/suppl/doi:10.1073/pnas.2011831117/-/DCSupplemental.

First published August 17, 2020.

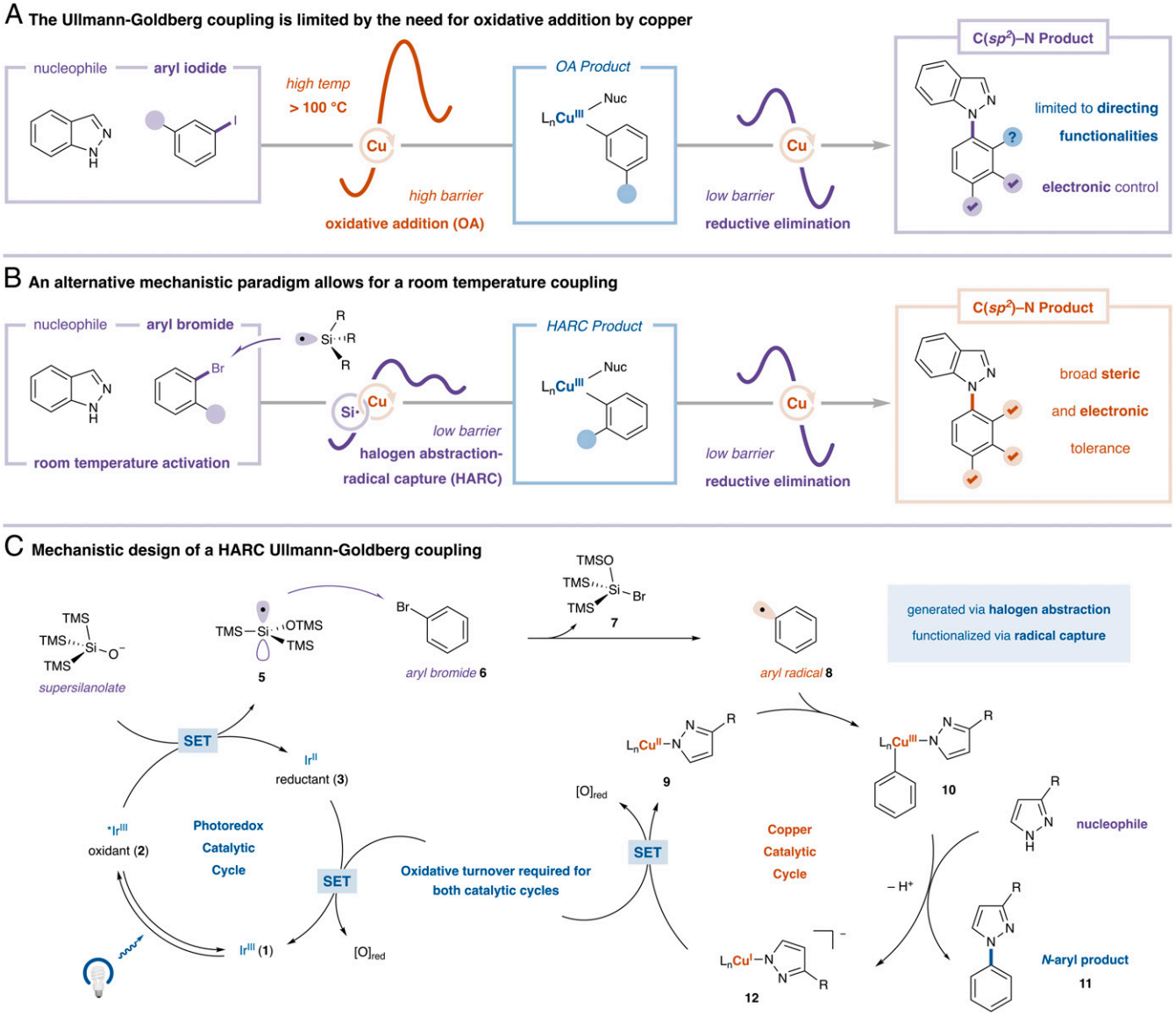

Fig. 1. Silanol-mediated copper metallaphotoredox catalysis enables a C(sp^2)–N coupling. (*A*) The Ullmann–Goldberg coupling features a high–barrier oxidative addition step overcome typically by high reaction temperatures, but this limits the aryl bromide scope to activated electrophiles. Sterically congested, nondirecting *ortho*- groups are not well tolerated under this activation mode. (*B*) A low-barrier HARC sequence is proposed that will deliver a similar intermediate at room temperature, while a facile reductive elimination step should furnish the C–N coupled product. This strategy will enable the use of sterically congested bromoarenes and those electronically deactivated toward oxidative addition. (*C*) Mechanistic design for silanol-mediated copper metallaphotoredox C(sp^2)–N coupling. Both the photoredox and copper cycles require exogeneous oxidant to turn over.

often problematic in traditional cross-couplings such as C(sp^3)- and C(sp^2)-trifluoromethyl groups (29, 30). Apart from the inherent utility of a catalytic CF_3-installation pathway, these studies also demonstrate that formal aryl and alkyl Cu(III) intermediates might be accessed (31) without the requirement of a high-barrier copper/aryl halide OA step.

Recently, we hypothesized that a copper–HARC mechanism would have significant implications for the Ullmann–Goldberg coupling. As shown in Fig. 1, the use of photogenerated supersilyl radicals, in conjunction with aryl bromides, NH-heteroaryls, and copper salts, should allow the formation of an HARC Cu(III) adduct that would be structurally and electronically identical to the corresponding thermal, OA Cu(III) adduct. However, access to this critical intermediate would involve two kinetically facile steps via an HARC pathway, while the thermal OA process requires a high-barrier copper/aryl halide insertion, a mechanistic distinction that carries significant implications for reaction scope, catalyst development, and substrate tolerance (7). More specifically, this HARC Ullmann–Goldberg coupling might allow 1) the implementation of a large array of *ortho*-substituted aryl halides that were previously problematic or inert due to steric interactions in the thermal copper-OA step, 2) the widescale use of aryl bromides in lieu of aryl iodides, the former being more broadly available in structurally diverse formats, 3) the use of simple copper salts [e.g., $Cu(acac)_2$, acac = acetylacetonate] in place of bespoke copper–ligand complexes, and 4) the removal of elevated reaction temperatures, which can often lead to substrate, reagent, or product decomposition. As a further benefit, we felt that catalyst optimization studies should be relatively straightforward with this HARC mechanism given that the copper catalyst is effectively decoupled from the bond-breaking step (halogen atom abstraction). In contrast, the electronic characteristics

of the copper catalyst are coupled to both steps in the thermal mechanism, a feature that can often place competing requirements on catalyst design (i.e., an electron-rich Cu species is preferred for OA, while an electron-deficient Cu salt is superior for the RE step).

Results and Discussion

Our mechanistic hypothesis for the proposed C(sp^2)–N coupling is detailed in Fig. 1*C*. Upon irradiation with visible light, excitation of photocatalyst [Ir(dFCF$_3$ppy)$_2$(5,5′-dCF$_3$bpy)](PF$_6$) (**1**) (dFCF$_3$ppy = 2-(2,4-difluorophenyl)-5-(trifluoromethyl)pyridine, 5,5′-dCF$_3$bpy = 5,5′-bis(trifluoromethyl)-2,2′-bipyridine) into the long-lived triplet $^*Ir^{III}$ complex **2** (τ = 279 ns) is expected (32). This excited state is highly oxidizing ($E_{1/2}^{red}[^*Ir^{III}/Ir^{II}]$ = +1.68 V versus the standard calomel electrode (SCE) in MeCN, ref. 32) and should readily undergo single-electron transfer (SET) with the supersilanolate derived from supersilanol ((TMS)$_3$SiOH, **4**) (E_{pa} [**4**/**4**$^{+\bullet}$] = +1.55 V versus SCE in MeCN, ref. 30) to give the ground-state Ir^{II} complex **3**. Upon oxidation and radical Brook rearrangement (33), the resulting nucleophilic silyl radical **5** should rapidly abstract a bromine atom from bromoarene **6** to generate the aryl radical **8** and silyl bromide **7**. This aryl radical should be rapidly captured by the Cu(II)-amido complex **9** (34) to form Cu(III) complex **10**, which upon facile reductive elimination would deliver the *N*-arylated Ullmann-Goldberg coupling product **11**. Ligation and deprotonation of the *N*-heterocyclic nucleophile would subsequently form the anionic Cu(I)–amido complex **12** (14), which upon oxidation by exogenous oxidant would reconstitute the Cu(II)–amido complex **9**. Oxidative turnover is also required for the photocatalytic cycle to return complex **3** to the ground-state Ir^{III} complex **1**. Notably, the photoredox and copper catalytic cycles are formally independent of one another given that this transformation is net oxidative.

Optimization studies performed with 3-phenylpyrazole (**13**) and 1-bromo-4-(trifluoromethyl)benzene (**14**) revealed that the use of photocatalyst **1**, commercially available Cu(acac)$_2$, supersilanol (**4**), and base were necessary to deliver the *N*-arylated coupling adduct **15** in useful yields (*SI Appendix*, Table S1). Notably, the coupling efficacy was initially shown to be dependent on both the identity of the oxidant and base, as well as the degree of light intensity. While potassium phosphate was initially found to be a suitable base, a low tolerance for photon intensity variation in these reactions led to a number of reproducibility concerns (40–88% yield, Fig. 2*A*). However, the use of 1,1,3,3-tetramethylguanidine (TMG), a homogeneous organic base, provided a protocol that is widely tolerant to light-emitting diode (LED) power while being consistently reproducible. Moreover, the recently popularized Integrated Photoreactor (as developed by Merck) (35) enabled these studies to be performed under tightly standardized conditions and with a high level of precision for photon exposure. It is important to note, however, that this new Ullmann–Goldberg coupling is equally competent using other blue LED sources (e.g., Kessil lamps). While a variety of oxidants were found to be ineffective for this coupling (Fig. 2*B*, 0–21% yield), the use of ambient air was found to be a privileged selection (80% yield). Last, the formation of aryl radical-derived side products, which include dehalogenation and dimerization adducts, could be mitigated via the control of stir rate and photon intensity, clearly demonstrating the importance of oxygen uptake rate (*SI Appendix*, Tables S2 and S3).

With these optimized conditions in hand, we sought to determine the breadth of *N*-heterocyclic ring systems that can readily undergo coupling via this dual catalytic pathway (Fig. 3). First, pyrazoles were found to participate with good to excellent yield depending on the electronics and substitution pattern of the azole ring (**16**–**21**, 45–87% yield). These examples nicely demonstrate that chlorine atoms do not undergo competitive abstraction with silyl radicals, while electrophilic moieties such as

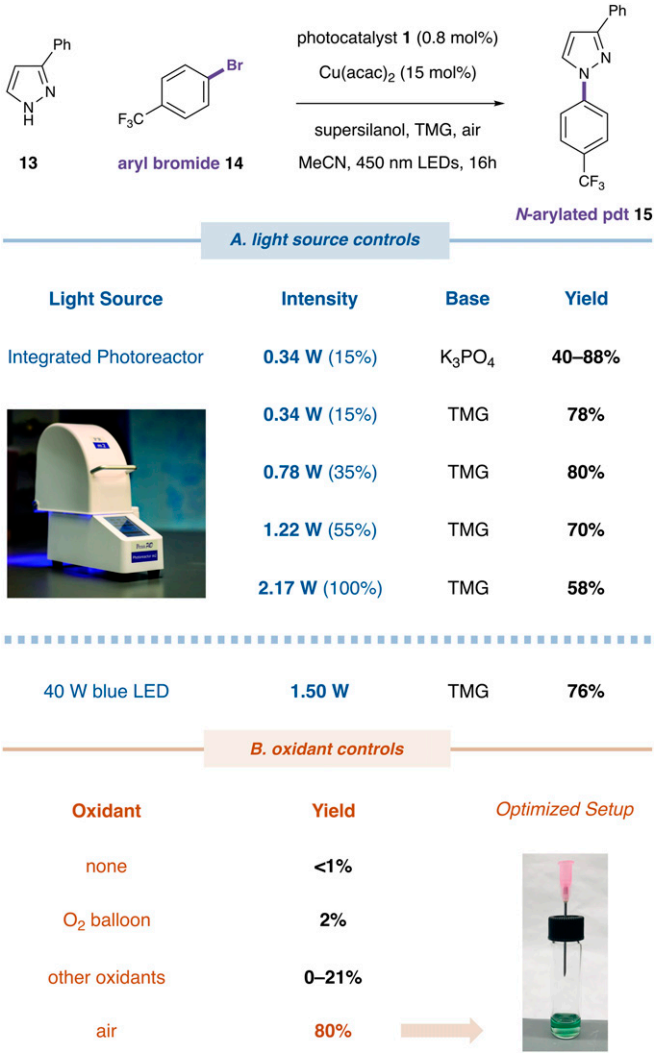

Fig. 2. Optimization and control reactions. (*A*) The Integrated Photoreactor allows for precise control of light intensity. Use of the organic base TMG provides a reproducible protocol broadly tolerant of LED power. The reaction is also competent with a 40-W blue LED light source (A160WE Tuna Blue Kessil lamp). (*B*) Air (introduced via an 18G needle) was shown to be a privileged oxidant. Other oxidants screened include (diacetoxyiodo)benzene (<1% yield), potassium persulfate (21% yield), 1-fluoro-2,4,6-trimethylpyridinium tetrafluoroborate (0% yield), and iodosobenzene (<1% yield). For full experimental details see *SI Appendix*.

esters are generically inert. Carbazole and indazoles were also shown to be competent nucleophiles (carbazole **22**, 66% yield, indazoles **23**–**26**, 64–70% yield), while basic heterocycles, such as 7-azaindoles and indoles, were also arylated under this catalytic manifold (7-azaindoles **27**–**29**, 49–70% yield, indoles **37** and **38**, 61% and 35% yield, respectively). A variety of 1,2,3- and 1,2,4-triazoles are competent nucleophilic partners in the protocol (**30** and **31**, both 40% yield), as were symmetrical benzimidazoles (**32** and **33**, 61 and 50% yield, respectively). In the case of unsymmetrical benzimidazoles we observed a mixture of regioisomers (**34**, 83% yield, 1.4:1 r.r.) due to the similar electronic and steric demands of both nitrogen centers. However, in the case of all other nonsymmetrical *N*-nucleophiles employed in this study, we observe only one regioisomer (as drawn), a remarkable selectivity we ascribe to the use of lower reaction temperatures throughout (4–25 °C).

We further tested this HARC/Ullmann–Goldberg protocol on heterocycles containing multiple nitrogens that have been widely

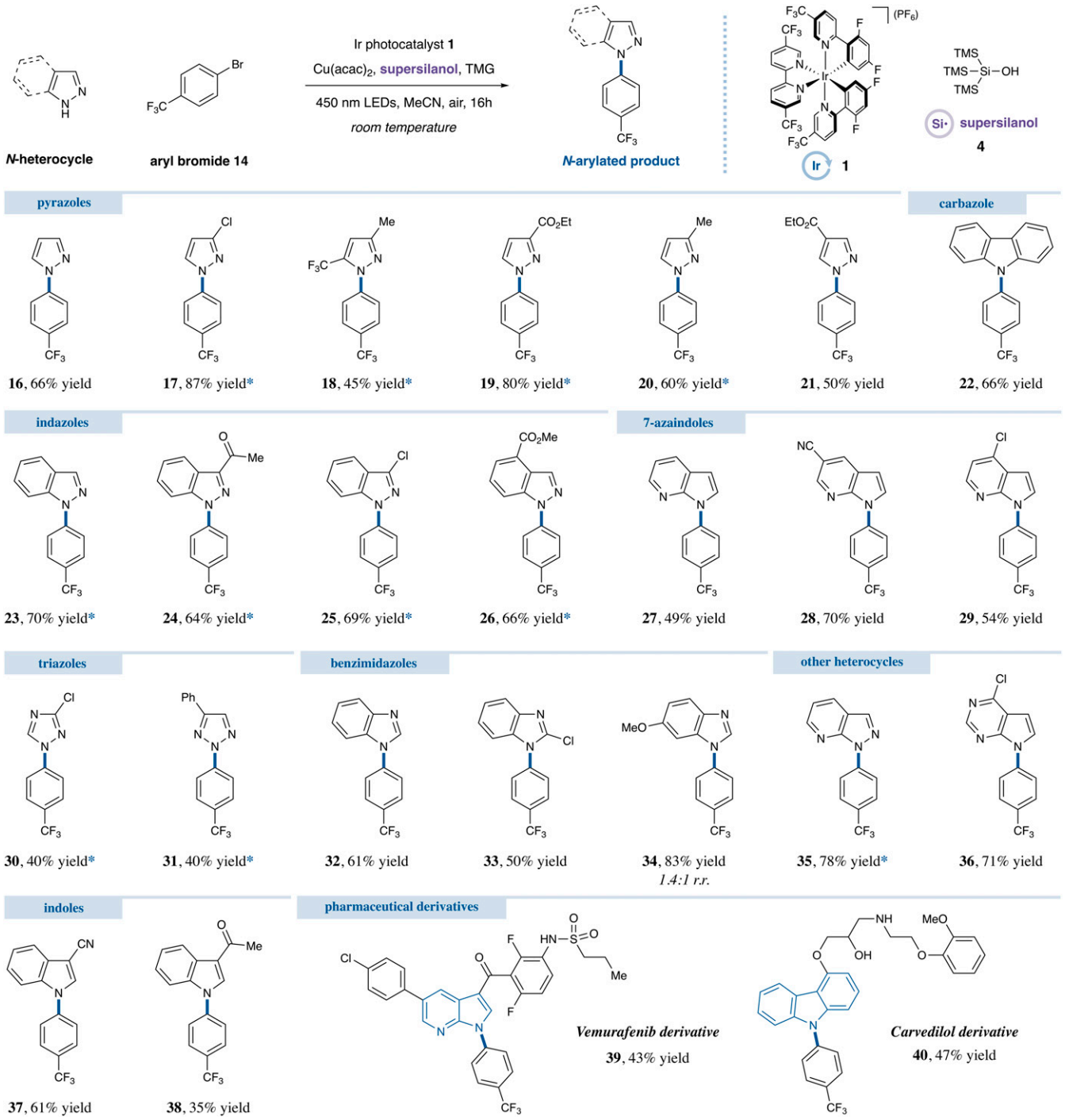

Fig. 3. Scope of nucleophiles in the photo-Ullmann–Goldberg coupling. Asterisks indicate that only one product was observed, despite the presence of multiple nucleophilic sites on the parent heterocycle. For full experimental details see *SI Appendix*.

employed as investigational pharmaceutical fragments. Gratifyingly, we found that a number of these nucleophiles underwent fragment coupling in good to excellent yield (**35** and **36**, 78% and 71% yield, respectively), further expanding the relevance of this Ullmann–Goldberg protocol to medicinal chemists. Moreover, the late-stage arylation of known pharmaceuticals containing multiple nucleophilic sites and coordinating functionalities such as sulfonamides and secondary amines has also been demonstrated (**39** and **40**, 43% and 47% yield, respectively). We envision that such chemoselectivity might be readily employed in combination with other established C–N coupling methods to allow for successive functionalization of *N*-nucleophilic sites on the same drug molecule.

We next explored the scope of the aryl bromide electrophiles in this new photo *N*-arylation protocol (Fig. 4). First, a large variety of electron-rich, -neutral, and -deficient bromoarenes were found to undergo successful coupling with *N*-aryl nucleophiles (**41**–**45**, 78–82% yield). Electronic diversity was also readily accommodated at both the *para*- and *meta*- positions across a spectrum of aryl rings (**46**–**51**, 64–85% yield). Moreover,

we were delighted to find that heteroaryl systems that can often disrupt the catalytic facility of copper via *N*–coordination were readily tolerated (**48**, 68% yield). For example, this coupling furnished *N*-arylated products in good to excellent yield for a variety of 2-pyridyl (**53**–**55**, 73–81% yield), 3-pyridyl (**56** and **57**, 62% and 74% yield, respectively), and 4-pyridyl (**58**, 76% yield) substrates. Moreover, pyrimidine (**59**, 64% yield), pyrazine (**60**, 78% yield), quinoline (**61**, 57% yield), and isoquinoline (**62**, 58% yield) are also readily implemented heterocyclic rings. Notably, this protocol was also successful in incorporating five-membered heteroaryl bromides (**63** and **64**, 57% and 52% yield, respectively), systems that can often be problematic for transition-metal catalysis, even at high temperatures (36, 37). Once again, we were able to extend the methodology to the late-stage diversification of two complex pharmaceutical aryl bromide scaffolds (**52** and **65**, 69% and 55% yield, respectively), highlighting the efficacy of the coupling in densely functionalized aryl bromides containing multiple *N*-nucleophilic centers. Also notable is that this method can be used to functionalize aryl iodides, as in the classic coupling reaction, but aryl chlorides and aryl triflates remain untouched (*SI Appendix*, Table S4). Last, as stated earlier, elevated temperatures are traditionally required when aryl bromides are employed in lieu of aryl iodides in Ullmann-Goldberg couplings. Remarkably, we have found that this photo-mediated *N*-arylation provides high levels of efficiency even when performed at *colder* temperatures (4 °C) across a broad series of aryl and heteroaryl bromides (**41**–**47**, 68–82% yield, **53** and **54**, 76% and 73% yield, respectively, **56** and

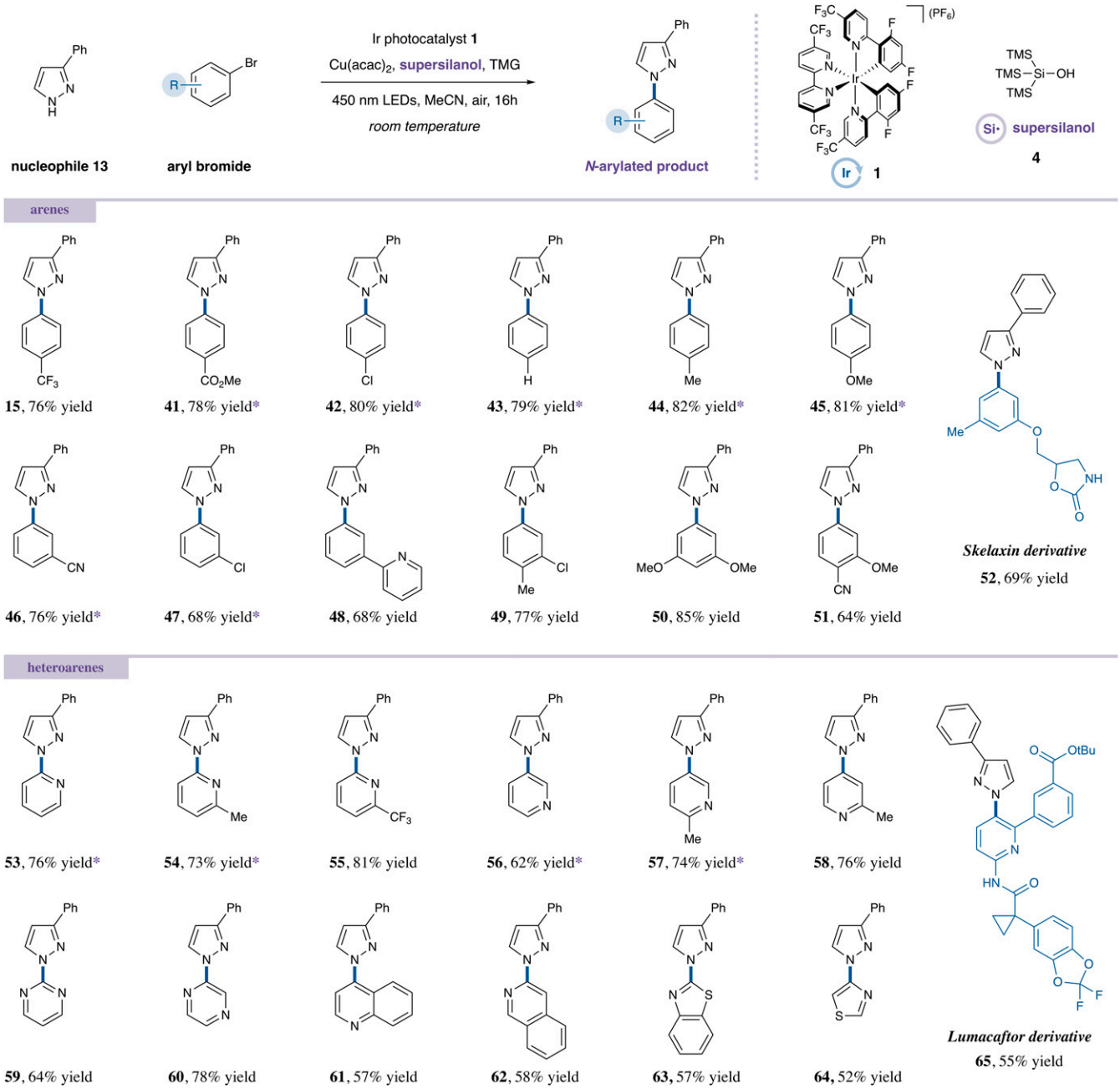

Fig. 4. Scope of bromoarenes in the arylation of *N*-heterocyclic nucleophiles. A diverse array of (hetero)aryl bromides were successfully activated by silyl radical toward copper-catalyzed C(sp^2)–N coupling, including pharmaceutically derived fragments. Asterisks indicate those reactions performed at 4 °C on 0.4-mmol scale. For full experimental details see *SI Appendix*.

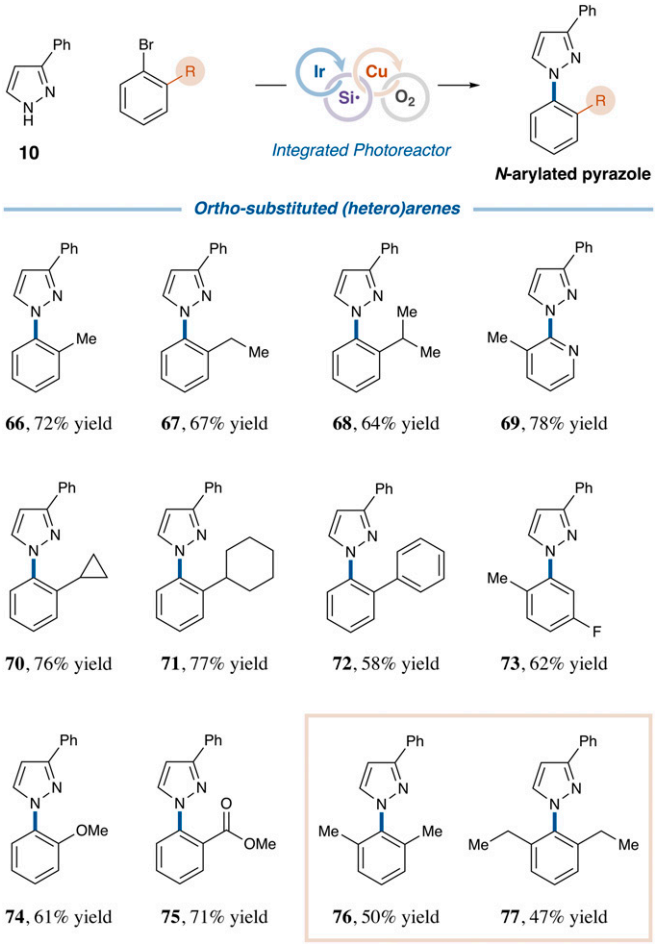

Fig. 5. Scope of 2- and 2,6-disubstituted aryl bromides. For full experimental details see *SI Appendix*.

57, 62% and 74% yield, respectively). This remarkable finding clearly underscores that the mechanism of this new C–N bond-forming reaction does not involve any high-barrier, thermally gated steps akin to copper oxidative addition.

Given that this photo-HARC mechanism is not encumbered by the kinetic and electronic issues that arise from the requirement of an oxidative addition step, we next questioned whether we could dramatically expand the scope of Ullmann–Goldberg couplings to include a wide array of *ortho*-substituted aryl bromides. Historically, chelating functionalities such as amides and carboxylates are among the few substituents tolerated at the *ortho* site of aryl electrophiles in the classical thermal protocol (7). In contrast, noncoordinating alkyl, aryl, or other bulky substituents are typically unsuccessful across a variety of reaction temperatures (38).

Using this copper metallaphotoredox protocol (Fig. 5), we were excited to find that *ortho* methyl-, ethyl-, and isopropyl-substituted bromobenzenes readily undergo coupling in good to excellent yield (**66**–**68**, 64–72% yield). Moreover, *ortho*-substituted heterocycles are also amenable to this functionalization method (**69**, 78% yield), and saturated rings of increasing size induce no discernible hindrance in the bond-forming step (**70** and **71**, 76% and 77% yield, respectively). Not surprisingly, substrates bearing coordinating functional groups were also tolerated (**74** and **75**, 61% and 71% yield, respectively) in accord with traditional pathways. Remarkably, this *N*-arylation proceeded with phenyl substituents at the *ortho* site, thereby delivering an elusive C(sp^2)–N triaryl adduct in excellent yield (**72**, 58% yield). Perhaps most notable, the method was also extended to the coupling of 2,6-bis-substituted aryl bromides (**76** and **77**) with only slight modifications to the stir rate, light intensity, and acetylacetonate ligand (50 and 47% yield, respectively). These latter examples further highlight the significance of decoupling the bond-breaking step from the bond-forming step in copper catalysis, given the impact of steric encumbrance on C(sp^2)–Br metal insertion versus silyl radical abstraction (39). In addition, application of this protocol to the diversification of a reported pharmaceutically active scaffold (38) resulted in the synthesis of *N*-arylated derivatives previously shown to be inaccessible via the classic thermal Ullmann–Goldberg coupling (*SI Appendix*, Figs. S3 and S4). Clearly, the potential benefits of an HARC mechanism when merged with transition-metal catalysis will likely expand beyond the realm of copper chemistry, and ongoing studies in our laboratory aim to exemplify such concepts.

Conclusions

The merger of photocatalytic silyl radical bromoarene activation with copper-catalyzed C(sp^2)–N_{het} coupling has facilitated the development of a general room-temperature protocol for the arylation of *N*-heterocyclic nucleophiles. This coupling exhibits a broad scope in both reaction partners, with multiple nucleophile classes and a range of electronically and sterically diverse aryl bromides exemplified. The ability of supersilanol to activate aryl bromides with steric bulk at the *ortho*- position, coupled with the ambient or low-temperature conditions, enables the potential for late-stage pharmaceutical functionalization. This method further demonstrates the capacity of metallaphotoredox to bypass difficult or problematic steps in traditional cross-coupling mechanisms in favor of kinetically facile alternatives. In this example, it renders a photo/Ullmann–Goldberg coupling that dramatically broadens the scope and late-stage applicability of the classic copper-catalyzed C–N coupling, while being accomplished without temperature burden.

Materials and Methods

General Procedure for C(sp^2)–N Coupling. To an oven-dried 40-mL vial charged with a flea stir bar we added nucleophile (0.25 mmol, 1.0 equiv.), aryl bromide (0.625 mmol, 2.5 equiv.), $Cu(acac)_2$ (0.0375 mmol, 15 mol%), and $[Ir(dFCF_3ppy)_2(5,5'\text{-}dCF_3bpy)](PF_6)$ (2.0 μmol, 0.8 mol%). Acetonitrile (99.9% Extra Dry Acros, 5 mL, 0.05 M) was added to the vial, followed by supersilanol (0.625 mmol, 2.5 equiv.) and TMG (0.75 mmol, 3 equiv.). The vial was capped and sonicated for 1 min to solubilize the reaction mixture. Then, the septum was pierced by an 18G needle, which was left in the septum for the duration of the reaction to allow for airflow without solvent evaporation. The vial was placed in the Integrated Photoreactor for 16 h under the following conditions: 5,000-rpm fan speed, 500-rpm stir rate, 35% light intensity. The final reaction mixture was diluted with ethyl acetate (10 mL) and stirred with KF (40 wt. % on alumina, 1.0 g) and tetrabutylammonium bromide (0.5 g) for at least 45 min, then filtered over Celite. The organic solution was washed with Na_2CO_3 (sat. aq.), water, and brine. The combined organics were dried over $MgSO_4$, filtered, and concentrated to yield the crude product. The product was purified via silica gel column chromatography.

Data Availability. All study data are included in the article and *SI Appendix*.

ACKNOWLEDGMENTS. The authors are grateful for financial support provided by the National Institute of General Medical Sciences (NIGMS), the NIH (under Award R35GM134897-01), the Princeton Catalysis Initiative, and kind gifts from Merck, Janssen, BMS, Genentech, Celgene, and Pfizer. M.N.L. acknowledges Princeton University for a first-year fellowship and also acknowledges Princeton University, E. Taylor, and the Taylor family for an Edward C. Taylor Fellowship. The content is solely the responsibility of the authors and does not necessarily represent the official views of NIGMS.

1. S. D. Roughley, A. M. Jordan, The medicinal chemist's toolbox: An analysis of reactions used in the pursuit of drug candidates. *J. Med. Chem.* **54**, 3451–3479 (2011).
2. G. Evano, N. Blanchard, M. Toumi, Copper-mediated coupling reactions and their applications in natural products and designed biomolecules synthesis. *Chem. Rev.* **108**, 3054–3131 (2008).
3. R. Dorel, C. P. Grugel, A. M. Haydl, The Buchwald-Hartwig amination after 25 years. *Angew. Chem. Int. Ed. Engl.* **58**, 17118–17129 (2019).
4. P. Ruiz-Castillo, S. L. Buchwald, Applications of palladium-catalyzed C–N cross-coupling reactions. *Chem. Rev.* **116**, 12564–12649 (2016).
5. F. Ullmann, Ueber eine neue Bildungseweise von Diphenylamin-derivaten. *Chem. Ber.* **36**, 2382–2384 (1903).
6. I. Goldberg, Ueber Phenylirungen bei Gegenwart von Kupfer als Katalysator. *Chem. Ber.* **39**, 1691–1692 (1906).
7. J. Lindley, Copper assisted nucleophilic substitution of aryl halogen. *Tetrahedron* **40**, 1433–1456 (1984).
8. D. S. Surry, S. L. Buchwald, Diamine ligands in copper-catalyzed reactions. *Chem. Sci.* **1**, 13–31 (2010).
9. D. Ma, Y. Zhang, J. Yao, S. Wu, F. Tao, Accelerating effect induced by the structure of α-amino acid in the copper-catalyzed coupling reaction of aryl halides with α-amino acids. Synthesis of benzolactam-V8. *J. Am. Chem. Soc.* **120**, 12459–12467 (1998).
10. H.-J. Cristau, P. P. Cellier, J.-F. Spindler, M. Taillefer, Mild conditions for copper-catalysed *N*-arylation of pyrazoles. *Eur. J. Org Chem.* **4**, 695–709 (2004).
11. E. R. Strieter, D. G. Blackmond, S. L. Buchwald, The role of chelating diamine ligands in the Goldberg reaction: A kinetic study on the copper-catalyzed amidation of aryl iodides. *J. Am. Chem. Soc.* **127**, 4120–4121 (2005).
12. S. E. Creutz, K. J. Lotito, G. C. Fu, J. C. Peters, Photoinduced Ullmann C-N coupling: Demonstrating the viability of a radical pathway. *Science* **338**, 647–651 (2012).
13. D. T. Ziegler *et al*., A versatile approach to Ullmann C-N couplings at room temperature: New families of nucleophiles and electrophiles for photoinduced, copper-catalyzed processes. *J. Am. Chem. Soc.* **135**, 13107–13112 (2013).
14. R. Giri *et al*., Mechanism of the Ullmann biaryl ether synthesis catalyzed by complexes of anionic ligands: Evidence for the reaction of iodoarenes with ligated anionic CuI intermediates. *J. Am. Chem. Soc.* **140**, 793–806 (2018).
15. H.-Z. Yu, Y.-Y. Jiang, Y. Fu, L. Liu, Alternative mechanistic explanation for ligand-dependent selectivities in copper-catalyzed *N*- and *O*-arylation reactions. *J. Am. Chem. Soc.* **132**, 18078–18091 (2010).
16. J. Twilton *et al*., The merger of transition metal and photocatalysis. *Nat. Rev. Chem.* **1**, 0052 (2017).
17. X. Zhang, D. W. C. MacMillan, Alcohols as latent coupling fragments for metallaphotoredox catalysis: sp^3–sp^2 cross-coupling of oxalates with aryl halides. *J. Am. Chem. Soc.* **138**, 13862–13865 (2016).
18. Z. Zuo *et al*., Dual catalysis. Merging photoredox with nickel catalysis: Coupling of α-carboxyl sp^3-carbons with aryl halides. *Science* **345**, 437–440 (2014).
19. Y. Liang, X. Zhang, D. W. C. MacMillan, Decarboxylative sp^3 C-N coupling via dual copper and photoredox catalysis. *Nature* **559**, 83–88 (2018).
20. P. J. Sarver *et al*., The merger of decatungstate and copper catalysis to enable aliphatic C(sp^3)-H trifluoromethylation. *Nat. Chem.* **12**, 459–467 (2020).
21. G. Ferraudi, Photochemical generation of metastable methylcopper complexes. Oxidation-reduction of methyl radicals by copper complexes. *Inorg. Chem.* **17**, 2506–2508 (1978).
22. M. Freiberg, D. Meyerstein, Reactions of aliphatic free radicals with copper cations in aqueous solution. Part 2.—Reactions with cupric ions: A pulse radiolysis study. *J. Chem. Soc. Faraday Trans. I* **76**, 1825–1837 (1980).
23. A. Casitas, X. Ribas, The role of organometallic copper(III) complexes in homogeneous catalysis. *Chem. Sci.* **4**, 2301–2318 (2013).
24. A. W. Dombrowski *et al*., Expanding the medicinal chemist toolbox: Comparing seven C(sp^2)–C(sp^3) cross-coupling methods by library synthesis. *ACS Med. Chem. Lett.* **11**, 597–604 (2020).
25. D. C. Blakemore *et al*., Organic synthesis provides opportunities to transform drug discovery. *Nat. Chem.* **10**, 383–394 (2018).
26. S. M. Hell *et al*., Silyl radical-mediated activation of sulfamoyl chlorides enables direct access to aliphatic sulfonamides from alkenes. *J. Am. Chem. Soc.* **142**, 720–725 (2020).
27. I. Grimm *et al*., Upscaling photoredox cross-coupling reactions in batch using immersion-well reactors. *Org. Proc. Res. Dev.* **24**, 1185–1193 (2020).
28. P. Zhang, C. C. Le, D. W. C. MacMillan, Silyl radical activation of alkyl halides in metallaphotoredox catalysis: A unique pathway for cross-electrophile coupling. *J. Am. Chem. Soc.* **138**, 8084–8087 (2016).
29. D. J. P. Kornfilt, D. W. C. MacMillan, Copper-catalyzed trifluoromethylation of alkyl bromides. *J. Am. Chem. Soc.* **141**, 6853–6858 (2019).
30. C. Le, T. Q. Chen, T. Liang, P. Zhang, D. W. C. MacMillan, A radical approach to the copper oxidative addition problem: Trifluoromethylation of bromoarenes. *Science* **360**, 1010–1014 (2018).
31. I. M. DiMucci *et al*., The myth of d8 copper(III). *J. Am. Chem. Soc.* **141**, 18508–18520 (2019).
32. G. J. Choi, Q. Zhu, D. C. Miller, C. J. Gu, R. R. Knowles, Catalytic alkylation of remote C-H bonds enabled by proton-coupled electron transfer. *Nature* **539**, 268–271 (2016).
33. M. Lucarini, E. Marchesi, G. F. Pedulli, C. Chatgilialoglu, Homolytic reactivity of group 14 organometallic hydrides towards nitroxides. *J. Org. Chem.* **63**, 1687–1693 (1998).
34. M. W. Johnson, K. I. Hannoun, Y. Tan, G. C. Fu, J. C. Peters, A mechanistic investigation of the photoinduced, copper-mediated cross-coupling of an aryl thiol with an aryl halide. *Chem. Sci.* **7**, 4091–4100 (2016).
35. C. C. Le *et al*., A general small-scale reactor to enable standardization and acceleration of photocatalytic reactions. *ACS Cent. Sci.* **3**, 647–653 (2017).
36. J. F. Hartwig, Evolution of a fourth generation catalyst for the amination and thioetherification of aryl halides. *Acc. Chem. Res.* **41**, 1534–1544 (2008).
37. P. J. Milner, Y. Yang, S. L. Buchwald, In-depth assessment of the palladium-catalyzed fluorination of five-membered heteroaryl bromides. *Organometallics* **34**, 4775–4780 (2015).
38. G. Dessole *et al*., Discovery of *N*-[(1-aryl-1*H*-indazol-5-yl)methyl]amides derivatives as smoothened antagonists for inhibition of the hedgehog pathway. *Bioorg. Med. Chem. Lett.* **19**, 4191–4195 (2009).
39. C. Chatgilialoglu, C. Ferreri, Y. Landais, V. I. Timokhin, Thirty years of $(TMS)_3SiH$: A milestone in radical-based synthetic chemistry. *Chem. Rev.* **118**, 6516–6572 (2018).